Application of Equal Area Criterion Conditions in the Time Domain for Out-of-Step Protection

Sumit Paudyal, *Student Member, IEEE*, Gokaraju Ramakrishna, *Member, IEEE*, and Mohindar S. Sachdev, *Life Fellow, IEEE*

***Abstract*—A new procedure for out-of-step protection by mapping the equal area criterion conditions to the time domain is proposed in this paper. The classification between stable and out-of-step swings is done using the accelerating and decelerating energies, which represents the area under the power-time curve. The proposed methodology is simple and overcomes some of the difficulties associated with the previous techniques. The proposed approach is based only on the local electrical quantities available at the relay location, and does not depend on the network configuration and parameters. The proposed algorithm has been tested on a single-machine infinite bus and a three-machine infinite bus system using software simulations. A digital prototype of the relay has also been implemented on the hardware and its performance has been assessed in a closed-loop mode using a real-time digital simulator. The simulation results and the hardware testing results confirm the validity of the approach presented.**

***Index Terms*—Equal area criterion, out-of-step, power swings, relays.**

I. Introduction

ELECTROMECHANCIAL oscillations in power systems happen due to an imbalance between input and output powers. Depending on the severity of a disturbance, the system may or may not return to a new stable condition. When the disturbance is severe, the oscillations do not damp out and lead to an unstable operating condition called out-of-step or loss-of-synchronism condition. The out-of-step relays are equipped to detect such conditions in the power system and disconnect a part of the system at preselected locations to bring the rest of the system back to a new stable condition [1], [2].

There are various techniques available in literature and in practice to detect out-of-step conditions. Most popular conventional out-of-step detection techniques use a distance relay with blinders in the impedance plane and a timer. The blinder and timer settings require knowledge of the fastest power swing, the normal operating region, and the possible swing frequencies, and are therefore system specific [1], [3]. Such techniques require extensive offline stability studies for obtaining the settings and their complexity increases when applied to multimachine systems. The performance also depends on the guidelines used for blinder and timer settings. The technique ensures better protection only in the worst case scenarios [4] and the performance is affected by the swing frequencies encountered [5].

Another technique monitors the rate of change of swing centre voltage (SCV) and compares it with a threshold value to discriminate between stable and out-of-step swings. With some approximations, the SCV is obtained locally from the voltage at the relay location, which consequently makes the SCV independent of power system parameters. However, the approximation is true only if the total system impedance angle is close to 90° [6]. For a multimachine system, the voltage measured at relay location does not give an accurate approximation of SCV. The technique also requires offline system stability studies to set the threshold value (rate of change of SCV), thereby making it system specific.

Reference [7] proposed out-of-step detection based on a neural network and [8] proposed the application of fuzzy logic using an adaptive network-based fuzzy interface (ANFIS) for out-of-step detection. In [7], the mechanical input power, generator kinetic energy deviation and average kinetic energy deviation are selected as inputs to the neural network. The neural network technique is applied to a three-machine Nine Bus system. The technique based on fuzzy logic explained in [8] uses machine angular frequency deviation and impedance angle measured at the machine terminals as inputs. These two techniques are able to make the decisions quickly for a new case, which has close resemblance to a known predefined case for which the algorithm is trained. However, the techniques need an enormous training effort to train for all possible swing scenarios. This makes the training process tedious and also the complexity increases as the system interconnections increase. The techniques make quick decisions only if adequately trained.

Reference [9] proposed the energy function criterion for loss-of-synchronism detection for a complex power system. During unstable swings, the entire power system oscillates in two groups, and series elements (called cutset) connect them. By evaluating the potential energy of the cutset, the stable and unstable conditions are predicted. The technique requires the measurements across all series elements as any of the series elements could form a cutset depending on the pre-disturbance conditions, type of disturbance, and its duration. Thus, to implement as an out-of-step algorithm, measurements across all series elements are required to find the cutset. This technique is difficult to implement as a protection algorithm because it is based on wide area information.

Manuscript received July 02, 2008; revised January 19, 2009, July 21, 2009. First published January 19, 2010; current version published March 24, 2010. Paper no. TPWRD-00521-2008.

S. Paudyal is with the Department of Electrical and Computer Engineering, University of Waterloo, Waterloo, ON N2L 3G1, Canada.

G. Ramakrishna and M.S. Sachdev are with the Department of Electrical and Computer Engineering, University of Saskatchewan, Saskatoon, S7N 5A9, Canada (email: sumit.paudyal@usask.ca; rama.krishna@usask.ca; sachdev@engr.usask.ca).

Digital Object Identifier 10.1109/TPWRD.2009.2032326

Reference [10] proposed an out-of-step detection technique based on the classical equal area criterion (EAC) in the power angle (δ) domain. The technique described requires pre- and post-disturbance power-angle (P_e-δ) curves of the system to be known to the relay. As the P_e-δ curves are dependent on the system configuration, many measurement and communication devices at various locations are required to gather the current system information.

This paper uses the above concept of EAC modified to the time domain. An out-of-step protection methodology is proposed using the concept of time domain EAC. The time domain EAC is based on the power-time (P_e-t) curve instead of the P_e-δ curves. The proposed technique uses only local output power (P_e) information and does not need any other power system parameter information (line impedances, equivalent machine parameters, etc). The electrical output power, P_e, over time is calculated from local voltage and current information measured at the relay location. The transient energy, which is the area under the P_e-t curve, is computed, and the swing is classified as stable or out-of-step based on the areas computed. The effectiveness of the proposed algorithm has been studied for a single-machine infinite bus (SMIB) and a three-machine infinite bus system using the PSCAD[1] software simulation tool. The simulation studies show that the proposed algorithm is simple and quick for detecting out-of-step conditions. The simulations results on three-machine Infinite Bus system also show that the proposed algorithm is effective for straightforward application to multimachine systems without any need for system reduction.

A digital prototype of the out-of-step relay has also been implemented on a digital signal processing (DSP) board, and closed-loop testing has been done using a real time digital simulator (RTDS).[2] The RTDS smulator is a digital electromagnetic transient power system simulator, which can be used for closed-loop testing of physical devices such as control and protection equipment. Successful closed-loop testing using the RTDS showed that the proposed algorithm could be equally effective on an actual power system, as the RTDS mimics the actual power system operating in real time [11], [12].

II. Proposed Algorithm

Fig. 1 shows an SMIB configuration, which is used to illustrate the proposed EAC in the time domain.

In Fig. 1, the sending end voltage (E_s) leads the receiving end voltage (E_R) by δ. The angle δ is referred to as the relative rotor angle or power angle. The steady state output power of the generator is P_e and is equal to the input mechanical power (P_m) to the generator. The system has two parallel lines, TL-I and TL-II, with impedances equal to X_1 and X_2, respectively.

A three phase fault is applied at the middle of TL-II. The fault is cleared with some delay by simultaneously opening the two breakers 'A' and 'B'. The transient response following a disturbance in the SMIB configuration is obtained if the swing equation (1) is solved using numerical integration techniques [13]

$$\frac{M}{\omega_s}\frac{d^2\delta}{dt^2} = P_m - P_e(\delta) \tag{1}$$

where M is the generator inertia constant and ω_s is the system frequency [13].

The advantage of EAC in δ domain is that it describes the stability of the system without solving the swing equation. The difficulties associated with EAC in δ domain to detect an out-of-step condition were discussed in the previous section. The proposed algorithm is based on P_e-t curve and this information can be obtained directly from the measurements at relay location. Thus the proposed algorithm does not require the solution of the swing equation to obtain the P_e-t curve.

Fig. 2 shows the P_e-δ curves for stable system. Fig. 3 shows the P_e-δ curves for an unstable system. The two curves are used to illustrate the EAC in δ domain. The P_e-t curves corresponding to the above two P_e-δ curves are shown in Figs. 4 and 5, and these curves are used to describe the proposed algorithm.

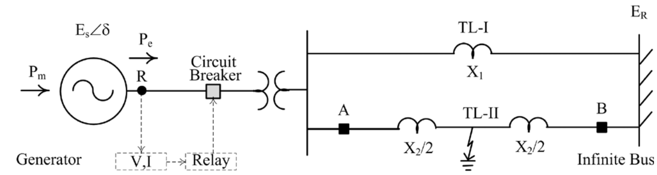

Fig. 1. Single-machine infinite bus system.

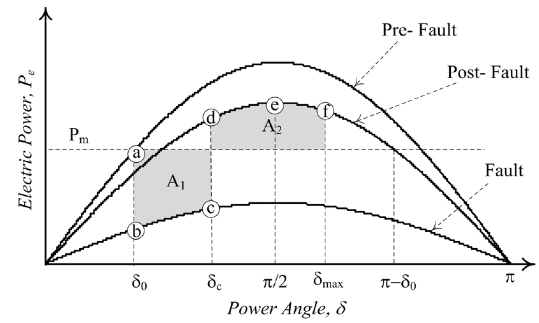

Fig. 2. P_e-δ curves illustrating a stable case.

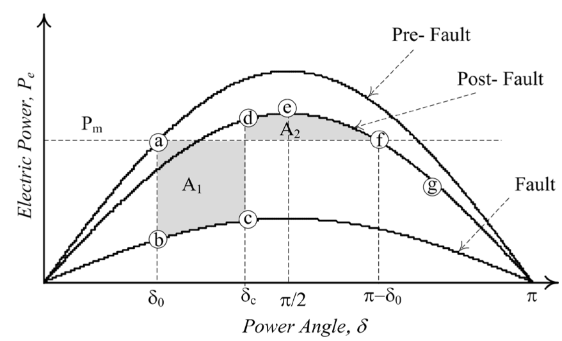

Fig. 3. P_e-δ curves illustrating an unstable case.

[1]PSCAD is a registered trademark of Manitoba HVDC Centre, Winnipeg, MB, Canada.

[2]RTDS is a registered trademark of RTDS Technologies, Inc., Winnipeg, MB, Canada.

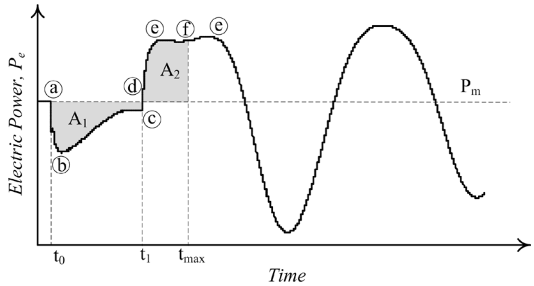

Fig. 4. P_e-t curve for a stable case.

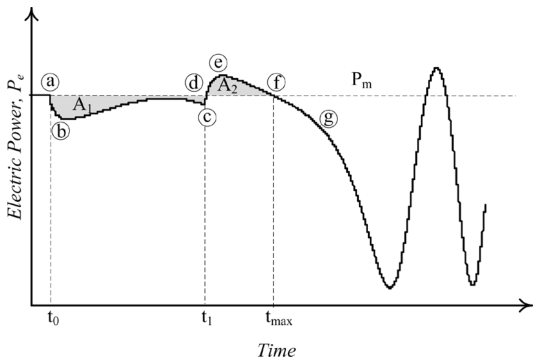

Fig. 5. P_e-t curve for an out-of-step case.

In Figs. 2 and 3, δ_0 represents the power angle before the fault, δ_c represents the power angle at the instance of fault clearing and $\delta_{\max}$ represents the maximum swing of the power angle. The EAC in δ domain tells that for a system to be stable, area A_1 is equal to area A_2, and area A_2 occurs before π-δ_0. For an unstable system, the area A_1 is greater than area A_2, and the area A_2 occurs at π-δ_0. The maximum swing of $\delta, \delta_{\max}$, for a stable swing is less than π-δ_0 [13].

The mathematical expressions to evaluate area A_1 and A_2 in time domain can be derived from the swing (1) [14]. If the speed deviation of the rotor is ω_Δ, then

$$\omega_\Delta = \omega(t) - \omega_s = \frac{d\delta}{dt} \tag{2}$$

where $\omega(\mathrm{t})$ is the speed of the rotor during transient.

From (1) and (2)

$$\frac{M}{\omega_s} d\omega_\Delta = (P_m - P_e)dt. \tag{3}$$

Integrating (3)

$$\frac{M}{\omega_S} \int d\omega_\Delta = \int (P_m - P_e)dt. \tag{4}$$

Area A_1 is obtained from (4) by setting the limit of integration from t_0 to t_1 (see Figs. 4 and 5). Where t_0 is the fault inception time (corresponding power angle is δ_0) and t_1 is the time when P_e exceeds P_m line. Note that at t_0, the speed deviation is zero because the speed of the rotor is synchronous speed

$$A_1 = \int_{t_0}^{t_1} (P_m - P_e(t))dt = \frac{M}{\omega_s}(\omega_\Delta|_{t_1} - \omega_\Delta|_0). \tag{5}$$

The area A_1 is positive as $P_m \geq P_e$ for $t = t_0$ to t_1. Similarly, area A_2 is obtained from (4) by setting the limit of integration from t_1 to $t_{\max}$.

$$A_2 = \int_{t_1}^{t_{\max}} (P_m - P_e(t))dt = \frac{M}{\omega_s}(\omega_\Delta|_{t_{\max}} - \omega_\Delta|_{t_1}) \tag{6}$$

where $t_{\max}$ is the time when $\delta = \delta_{\max}$. The area A_2 is negative as $P_m \leq P_e$ for $t = t_1$ to $t_{\max}$. For a stable system, at $t_{\max}$, the speed of the rotor is synchronous speed, so the speed deviation is zero. For an out-of-step condition, the speed of the rotor at $t_{\max}$ is greater than the synchronous speed. Thus, the total area for stable and out-of-step conditions from (5) and (6) is given as follows:

For a stable condition

$$A = A_1 + A_2 = \int_{t_0}^{t_{\max}} (P_m - P_e(t))dt = 0. \tag{7}$$

For an out-of-step condition

$$A = A_1 + A_2 = \int_{t_0}^{t_{\max}} (P_m - P_e(t))dt > 0. \tag{8}$$

Equations (7) and (8) are the expressions for EAC in time domain, which tells that during the transient, if area A_1 and A_2 under the P_e-t curve are equal, the system becomes stable. But if area A_1 becomes greater than area A_2, the system goes to an out-of-step condition. The area under the P_e-t curve represents energy. Thus, this concept can be referred to as the energy equilibrium criterion in the time domain. A balance of transient energy results in a stable swing whereas an unbalance of transient energy results in an out-of-step swing.

Integrations in (7) and (8) are approximated by summation and P_m is set to P_e before the fault inception. The time limits are also expressed in terms of P_e. Thus, for a stable condition, the sum of two areas A_1 and A_2 becomes

$$A = \sum_{t_0}^{t_{\max}} (P_e(t)|_{t_0 - \Delta t} - P_e(t))\Delta t = 0. \tag{9}$$

For an out-of-step condition

$$A = \sum_{t_0}^{t_{\max}} (P_e(t)|_{t_0 - \Delta t} - P_e(t))\Delta t > 0 \tag{10}$$

where

t_0	time when $P_e(t) < P_e(t)|_{t-\Delta t}$ first occurs;
$t_{\max}$	time when $A|_t = 0$ (stable) or time when

$$P_e(t)|_{t-\Delta t} > P_e(t)|_{t_0 - \Delta t} \text{ and } P_e(t) \leq P_e(t)|_{t_0 - \Delta t} (\text{out–of–step})$$

In (9) and (10), Δt represents a sampling interval, the time after which a new value of P_e is available to the out-of-step relay. Equation (9) and the limit $t_{\max}$ for stable case do not become exactly equal to zero because of the approximation of integration by summation. They are modified as

$$A=\sum_{t_0}^{t_{\max}}\left(P(t)_e|_{t_0-\Delta t}-P_e(t)\right)\Delta t\le 0. \tag{11}$$

$t_{\max}$ time when $A|_{t-\Delta t}>0$ and $A|_t\le 0$ (Stable).

Equations (10) and (11) along with the conditions for t_0 and $t_{\max}$ form the proposed algorithm for out-of-step detection. Based on the proposed algorithm, a decision regarding a stable or out-of-step condition is always made at $t_{\max}$ (time corresponding to $\delta_{\max}$) with an error of Δt or less.

The generators are considered lossless in (9). However, in an actual system, the P_e calculated at fault inception from the local measurements has to be corrected for losses and other loads (house load etc) connected to the generator.

In the studies, the presence of instability is assumed when the maximum disturbance magnitude (change in P_e from the original value) is greater than 10%. This way, further calculations due to noise and other dynamic oscillations, are avoided. In a practical implementation, the technique will be used in conjunction with a relay starter element, so that it operates only for fault situations.

The instability criterion discussed in this section shows that the method is simple to apply and is well-suited for applying it for out-of-step protection purposes. The following sections give the simulation and hardware implementation results using the proposed technique.

III. Software Simulations

The proposed algorithm has been tested on two power system models: an SMIB and a three-machine infinite bus system.

A. SMIB Simulation

A power system as shown in Fig. 1 is used to test the proposed algorithm on an SMIB configuration. The power system parameters are given in the Appendix [15]. An out-of-step relay is located at 'R.' At 'R,' voltage and current information of three phases are measured and electric output power of the generator (P_e) is calculated. A discrete Fourier transform (DFT) technique is used for estimating the values of voltage and current phasors from the instantaneous values of voltage and current measurements. The pre-fault power angle (δ_0) is set at 30°. A three phase fault is applied at the middle of TL-II and four different simulations are carried out with fault duration times of 0.167, 0.20, 0.233 and 0.267 s. Power system transient simulation tool PSCAD is chosen for the simulation with a simulation time step of 50 μs [16]. The fault duration times of 0.167 and 0.20 s make the system stable whereas the fault duration times of 0.233 and 0.267 s result in an out-of-step condition. The P-t curves are shown in Fig. 6–9 and results are summarized in Table I.

The simulation results show that the proposed algorithm discriminates the stable and out-of-step swings effectively. The cases 1 and 2 are decided as stable swing as the total area A becomes zero. In cases 3 and 4; total area A becomes 0.034 and 0.051 p.u.-s respectively. Thus, these cases are decided as out of step.

The performance of the proposed relay was compared to a concentric rectangle scheme used in practice [17]. In a concentric rectangle scheme, the time taken by impedance seen by the relay to traverse inner and outer rectangles is compared with the preset time to discriminate between a fault and a swing. If the swing locus traverses inner and outer rectangles in less than the pre-set time, the disturbance is a fault. If the locus enters the

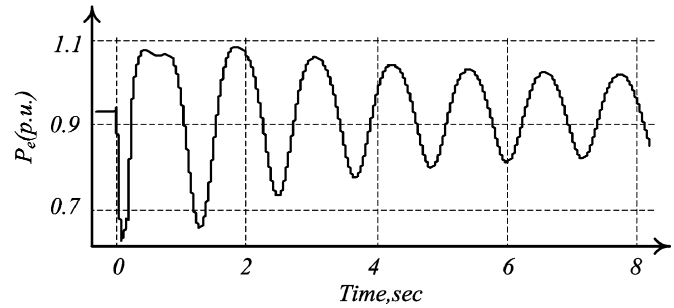

Fig. 6. $\mathrm{P_e}$-t curve for $\delta_0=30°$ and fault cleared after 0.167 s.

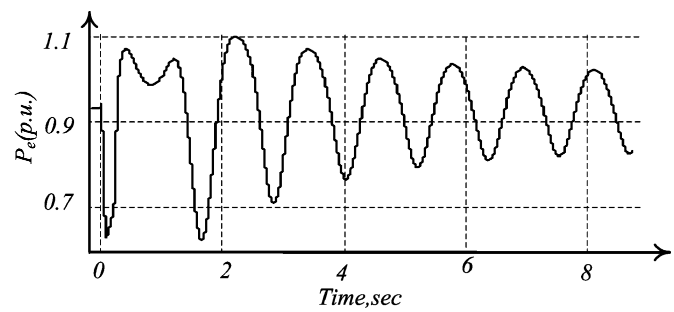

Fig. 7. $\mathrm{P_e}$-t curve for $\delta_0=30°$ and fault cleared after 0.20 s.

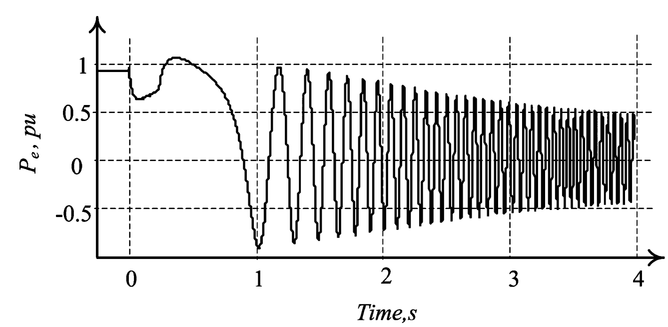

Fig. 8. $\mathrm{P_e}$-t curve for $\delta_0=30°$ and fault cleared after 0.233 s.

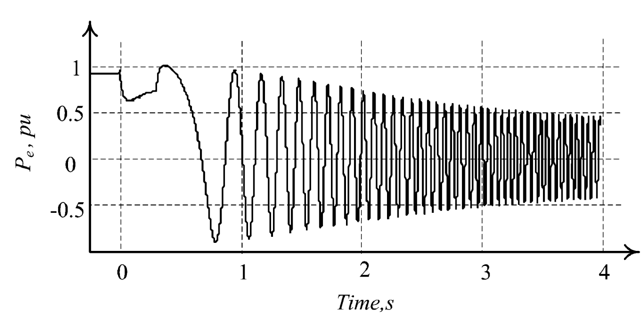

Fig. 9. $\mathrm{P_e}$-t curve for $\delta_0=30°$ and fault cleared after 0.267 s.

TABLE I
SUMMARY OF STABLE AND OUT-OF-STEP SWINGS ON AN SMIB SYSTEM

Case	**1**	**2**	**3**	**4**
Power Angle (δ_0)	30°	30°	30°	30°
Fault Duration Time, s	0.167	0.20	0.233	0.267
Area (A_1) pu-s	0.048	0.054	0.061	0.067
Area (A_2) pu-s	-0.048	-0.054	-0.027	-0.016
$A=A_1+A_2$	0	0	0.034	0.051
Decision Time, s	0.640	0.850	0.598	0.504
Decision	Stable	Stable	OS	OS

OS: Out-of-step

outer rectangle and takes more time than the preset time to cross the inner rectangle, then it is an out-of-step condition. If the swing locus crosses the outer rectangle but does not cross the inner rectangle, the swing is a stable swing. Commercial relay manufacturers use maximum load flow and the maximum swing angle that the power system can tolerate to determine the outer and inner blinder characteristics. Detailed guidelines used for relay settings are described in [17].

The out-of-step detection times using the two techniques were compared for the two worst case scenarios (cases 3 and 4) in Table I. For case 3, the concentric rectangular scheme took 0.618 s from the inception of fault. The swing alone took 27.5 cycles (0.458 s) to traverse between the two concentric rectangles. For this case, the proposed algorithm took 0.598 s from the inception of fault to detect that it is an out-of-step condition.

For case 4, the fault clearing time was increased to 16 cycles (0.26 s). The swing locus took 20.98 cycles (0.349 s) to traverse between the two concentric rectangles and the decision that it is out-of-step was obtained at 0.524 s whereas the proposed algorithm took 0.504 s to make the decision.

The above results show that the proposed algorithm is fast and effective for discriminating between stable and out-of-step conditions on an SMIB system. As stated earlier, P_e is calculated from the local voltage and current measurements at 'R,' without solving the swing equation. The out-of-step relay only requires the P_e information; it does not require the network parameters information or the network structure. This makes the application of the algorithm simple and straightforward.

B. Three-Machine Infinite Bus Simulation

A three-machine Infinite Bus system as shown in Fig. 10 is considered to illustrate the effectiveness of the proposed technique for a multimachine system. The parameters of the power system are given in the Appendix. The generator *Gen1* is equipped with an out-of-step relay at location 'R.' The voltage and current measurements at 'R' are used to calculate the P_e out of *Gen1*. A three phase fault is applied at *Bus 2* and four different simulations are reported here with: 1) $P_m = 0.984$ p.u. and fault duration of 0.1 s; 2) $P_m = 0.877$ p.u. and fault duration of 0.25 s; 3) $P_m = 0.984$ p.u. and fault duration of 0.25 s; and 4) $P_m = 0.877$ p.u. and a fault duration of 0.30 s. The P-t curves for the four cases are shown in Fig. 11–14. The calculated areas and the decisions made are summarized in Table II.

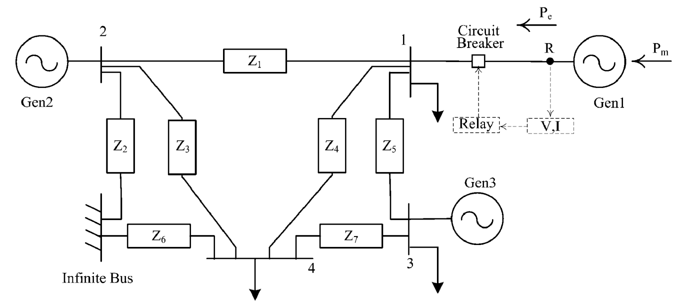

Fig. 10. Three-machine infinite bus system.

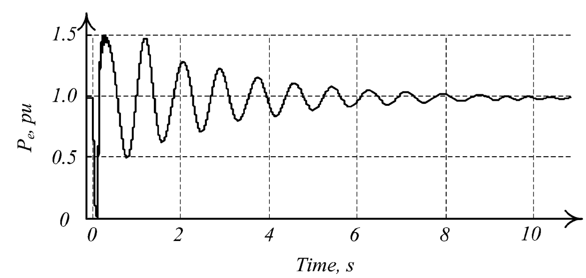

Fig. 11. P_e-t curve of Gen1 for $P_m = 0.984$ p.u. and fault cleared after 0.1 s.

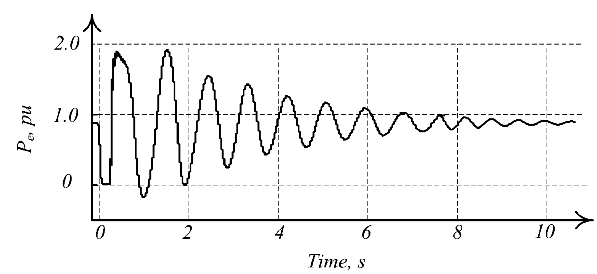

Fig. 12. P_e-t curve of Gen1 for $P_m = 0.877$ p.u. and fault cleared after 0.25 s.

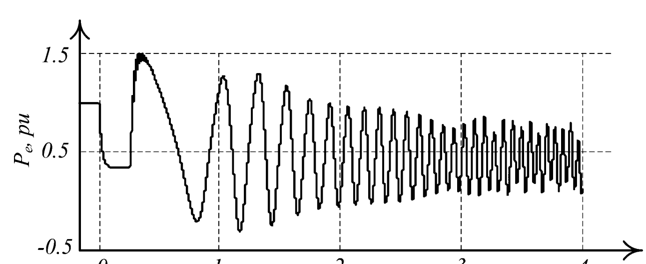

Fig. 13. P_e-t curve of Gen1 for $P_m = 0.984$ p.u. and fault cleared after 0.25 s.

The first two cases are decided as stable swing because the total area A calculated is zero. In the other two cases, area A is greater than zero. Consequently, out-of-step decisions are made.

To study the effect of pure local mode oscillations on the proposed algorithm, a load increase of 0.15 p.u. was applied at bus 3, and at the same instant, a decrease in load by 0.15 p.u. was applied at bus 1. The P-t curve for this simulation case is shown in Fig. 15. The base MVA for p.u. calculations was chosen equal to 555 MVA. The figure shows that a ± 0.15 p.u. local area load change produces a stable swing. The frequency of oscillation was found to be approximately equal to 2.05 Hz.

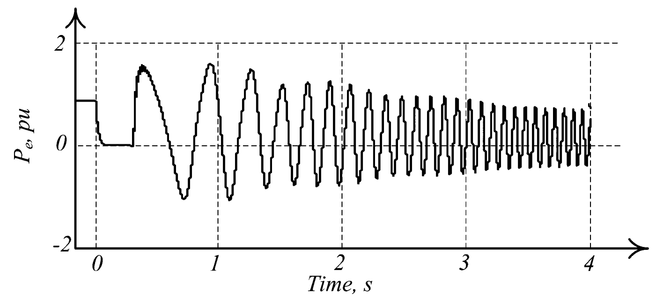

Fig. 14. $\mathrm{P_e}$-t curve of Gen1 for $\mathrm{P_m} = 0.877$ p.u. and fault cleared after 0.30 s.

TABLE II
SUMMARY OF STABLE AND OUT-OF-STEP SWINGS
(THREE-MACHINE INFINITE BUS SYSTEM)

Case	5	6	7	8
Input Power (P_m), pu	0.984	0.877	0.984	0.877
Fault Duration Time, s	0.1	0.25	0.25	0.30
Area (A_1), pu-s	0.0895	0.2127	0.2391	0.2531
Area (A_2), pu-s	-0.0895	-0.2127	-0.1204	-0.0774
Decision Time, s	0.346	0.519	0.536	0.500
Decision	Stable	Stable	OS	OS

OS: Out-of-step

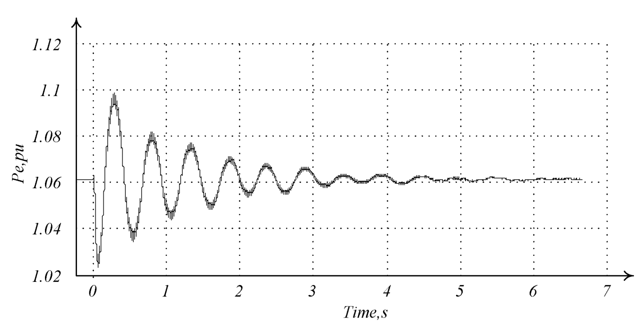

Fig. 15. $\mathrm{P_e}$-t curve of Gen1 for a ± 0.15 p.u. local area load change.

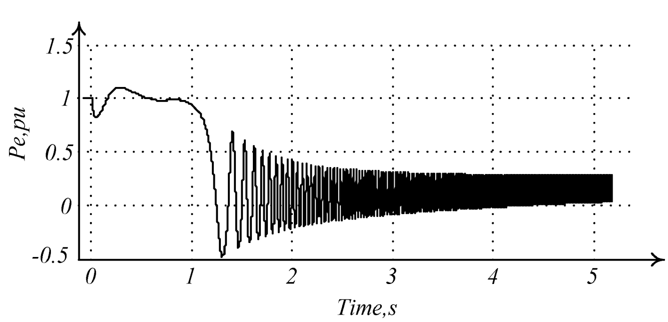

Fig. 16. $\mathrm{P_e}$-t curve of Gen1 for a ± 0.5 p.u. local area load change.

To excite an unstable case due to local mode oscillations, the load at bus 3 was increased by 0.5 p.u., and at the same time, a 0.5 p.u. decrease in load was applied at bus 1. The P-t curve for this simulation case is shown in Fig. 16. The graph shows that this is an unstable case. The initial frequency of oscillation in this case was found to be approximately equal to 2.09 Hz. A summary of results for *Gen1* due to local mode oscillations is given in Table III.

Table IV gives a summary of results (due to local mode disturbances) when an out-of-step relay is located at *Gen3*. The base MVA used for p.u. calculations is 66 MVA. Case 12 is a stable case whereas cases 13 and 14 are unstable cases.

TABLE III
LOCAL MODE OSCILLATION STUDIES FOR GEN1
(THREE-MACHINE INFINITE BUS SYSTEM)

Case	9	10	11
Input Power (P_m), pu	1.059(Gen1)	1.01(Gen1)	0.877(Gen1)
Load change	-0.15 pu @Bus1 +0.15 pu @ Bus 3	-0.5 pu @Bus1 +0.5 pu @ Bus 3	Fault @ 70% of TL between Bus 1 and 3 for 0.1 sec
Area (A_1), pu-s	0.0327	0.02040	0.45434
Area (A_2), pu-s	-0.0327	-0.0180	-0.02059
Decision Time, s	0.2815	0.544	0.921
Decision	Stable	OS	OS
Initial frequency, Hz	2.05	2.09	2.32
Frequency after 4sec, Hz	1.89	19.86	8.82

OS: Out-of-step

TABLE IV
LOCAL MODE OSCILLATION STUDIES FOR GEN3
(THREE-MACHINE INFINITE BUS SYSTEM)

Case	12	13	14
Input Power (P_m), pu	0.476(Gen3)	1.010(Gen3)	0.5196(Gen3)
Load change	+1.26 pu @Bus1 -1.26 pu @ Bus 3	4.2 pu @Bus1 -2.1 pu @ Bus 3 -2.1 pu @ Bus 4	Fault @ 70% of TL between Bus 1 and 3 for 0.1 sec
Area (A_1), pu-s	0.0137	0.00174	0.26545
Area (A_2), pu-s	-0.0137	-0.00013	-0.10429
Decision Time, s	0.149	0.233	0.931
Decision	Stable	OS	OS
Initial frequency ,Hz	2.8	4.54	2.419
Frequency after 4sec, Hz	2.54	25.77	8.33

OS: Out-of-step

The results show that the proposed algorithm is not only effective on an SMIB system, but it is equally effective on an interconnected power system. The application of this technique is straightforward even for a large power system and avoids the need for any cumbersome network reduction techniques, such as center of inertia or center of angle technique [18], [19].

IV. HARDWARE IMPLEMENTATION AND CLOSED-LOOP TESTING

The simulation results in the previous section showed that the algorithm is effective for discriminating between stable and out-of-step swings. This section describes the implementation and closed-loop testing of a digital out-of-step relay based on the proposed algorithm.

A. Digital Out-of-Step Relay Model

The main hardware used is the RTDS and ADSP-BF533 EZ LITE-KIT board (from Analog Devices).[3] The details of the hardware are given in the Appendix [11], [12], [20].

A relay model is built on an ADSP-BF533 EZ LITE-KIT board and a power system is modeled on RTDS to test the proposed algorithm in real time. The simplified diagram of the relay and power system models and their interfacing is shown in Fig. 17. The three phase terminal voltages and currents of the generator are fed to the ADSP-BF533 EZ LITE-KIT board through

[3]Analog Devices is a registered trademark of Analog Devices, Inc.

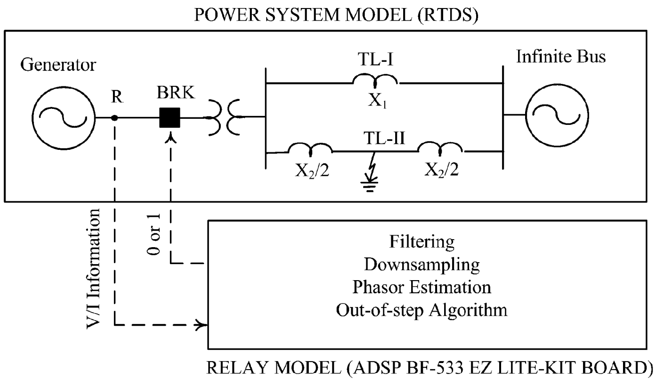

Fig. 17. Relay and power system model and their connections.

the RTDS analog output ports. The hardware relay's digital outputs are "0" for a stable system and "1" for out-of-step. This signal is fed back to the RTDS through its digital input port and controls the status of breaker BRK. If it is "1", it trips the breaker and disconnects the generator from the infinite bus.

The relay model developed on the ADSP-BF533 EZ LITE-KIT board has four blocks: filtering, down-sampling, phasor estimation and the out-of-step algorithm as shown in Fig. 17. A fifth order infinite impulse response (IIR) Butterworth filter is used to filter out the noise seen in the signals tapped from the RTDS. The cutoff frequency of the filter is set at 65 Hz (408.4 rad/s). The DSP board samples at 48000 samples/second. But for this study only 16 samples/cycle are used, thus Downsampling block is required. As the input signals are of 60 Hz, the input signals should be sampled at 960 samples/second. Thus this block downsamples the input signals by $50 (= 48000/960)$ times. Discrete Fourier transform (DFT) is used for the phasor estimation of voltage and current signals. The DFT technique requires two orthogonal signals (sine and cosine) of 60 Hz signal sampled at the same rate as the input signals (i.e., 16 samples/cycle), which gives a sampling interval of 0.00104 s. The out-of-step algorithm block uses the voltage and current phasors and calculates P_e. This block employs the out-of-step algorithm proposed in (10) and (11) and outputs '0' for stable or '1' for out-of-step condition.

B. Closed-Loop Testing Results

The RTDS and ADSP-BF533 EZ LITE-KIT board are connected as shown in Fig. 17. In the RTDS power system model, various swing conditions are generated by setting the pre-fault power angle (δ_0) of the generator at different values (35°, 40° and 45°); by applying various types of fault (three phase, line-ground and line-line) at the middle of the transmission line (TL-II) and by varying the fault duration time.

First the δ_0 is set at 35°, three phase fault is applied at the middle of TL-II and fault duration time is set at 0.22, 0.26, 0.271, 0.272 and 0.28 s, respectively. The P_e-t curves are shown in Figs. 18–22. The first three fault duration times make the system stable and the other two make the system to go out of step. When the fault duration time is increased from 0.271 to 0.272 s, the swing becomes out of step from being stable; these cases depict the marginally stable and unstable cases and are discriminated well by the relay. The summary of the areas A_1 and A_2 calculated and the decision and times are listed in Table V.

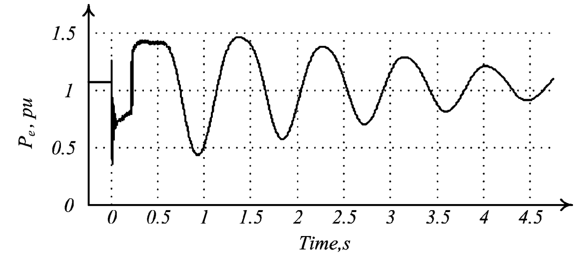

Fig. 18. $\mathrm{P_e}$-t curve for $\delta_0 = 35°$ and fault cleared after 0.22 s.

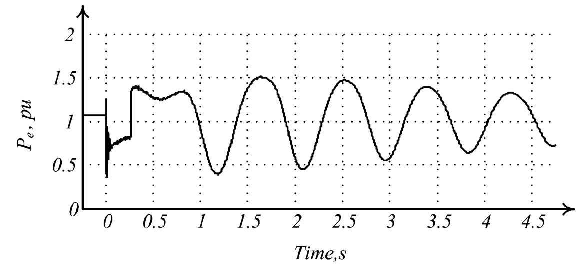

Fig. 19. $\mathrm{P_e}$-t curve for $\delta_0 = 35°$ and fault cleared after 0.26 s.

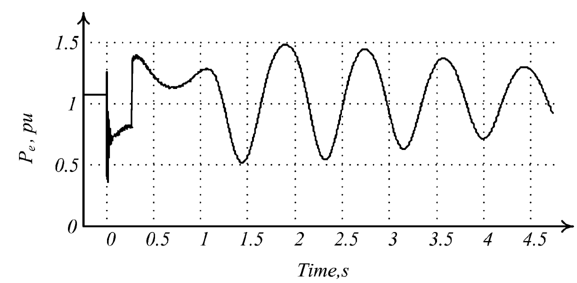

Fig. 20. $\mathrm{P_e}$-t curve for $\delta_0 = 35°$ and fault cleared after 0.271 s.

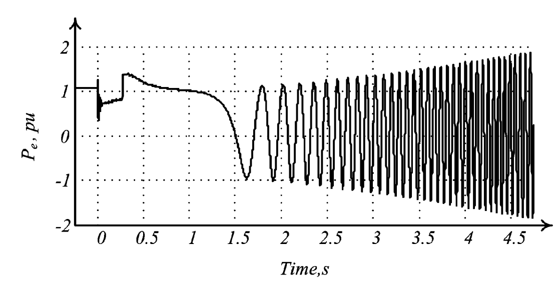

Fig. 21. $\mathrm{P_e}$-t curve for $\delta_0 = 35°$ and fault cleared after 0.272 s.

Two of the hardware simulation scenarios discussed above (i.e., corresponding to fault duration times of 0.22 s and 0.272 s) were also simulated using PSCAD, and the results are given in Figs. 23 and 24. Table VI gives a comparison of the two sets of results obtained. When the fault duration is 0.22 s, the hardware simulation gives a stable decision at 0.4794 s, whereas with the software simulation, the same decision is obtained at 0.4784 s. When the fault duration time is 0.272 s, out-of-step decisions are obtained using hardware and software simulations at 0.6957 s and 0.6895 s, respectively. The decision times obtained verify that the hardware and software results are in close agreement.

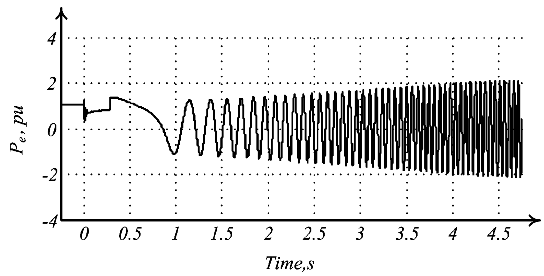

Fig. 22. P_e-t curve for $\delta_0 = 35°$ and fault cleared after 0.278 s.

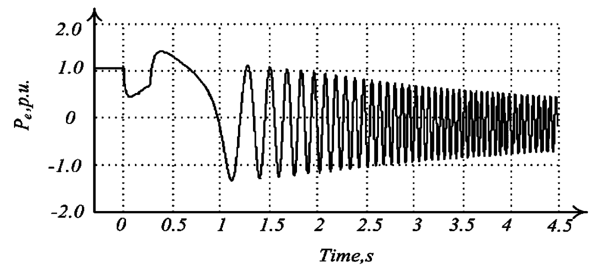

Fig. 24. P_e-t curve for $\delta_0 = 35°$ and fault cleared after 0.272 s (PSCAD results).

TABLE V
SUMMARY OF CLOSED-LOOP TESTING RESULTS FOR PRE-FAULT $\delta = 35°$ AND THE THREE PHASE FAULT APPLIED

Case	*15*	*16*	*17*	*18*	*19*
Fault Duration Time, s	0.22	0.26	0.271	0.272	0.28
Fault Duration Samples	211	250	260	261	269
Area (A_1), in 10^9	7.674	9.083	8.994	8.585	10.007
Area (A_2), in 10^9	7.676	9.098	8.995	6.451	0.355
Decision	Stable	Stable	Stable	OS	OS
Decision Made at Sample	461	707	944	669	495
Decision Time, s	0.4794	0.7353	0.9817	0.6957	0.5148

OS: Out-of-step

TABLE VI
COMPARISON OF RESULTS OBTAINED FROM HARDWARE AND SOFTWARE SIMULATIONS

Case	*20*	*21*	*22*	*23*
Simulation Tool	Hardware	Software	Hardware	Software
Power Angle (δ_0)	35°	35°	35°	35°
Fault Duration Time, s	0.22	0.22	0.272	0.272
Area (A_1)	7.674×10^9	0.058	8.585×10^9	0.071
Area (A_2)	7.676×10^9	0.058	6.451×10^9	0.055
Decision	Stable	Stable	OS	OS
Decision Time, s	0.4794	0.4784	0.6957	0.6895

OS: Out-of-step

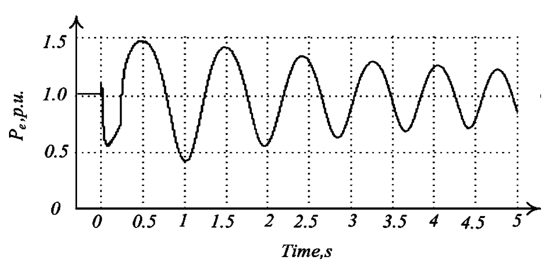

Fig. 23. P_e-t curve for $\delta_0 = 35°$ and fault cleared after 0.22 s (PSCAD results).

TABLE VII
SUMMARY OF CLOSED-LOOP TESTING RESULTS FOR PRE-FAULT $\delta = 40°$ AND THE LINE TO LINE FAULT APPLIED

Case	*24*	*25*	*26*	*27*	*28*
Fault Duration Time, s	0.4	0.42	0.435	0.436	0.437
Fault Duration Samples	384	403	418	419	420
Area (A_1), in 10^9	6.630	6.846	6.913	6.961	6.981
Area (A_2), in 10^9	6.631	6.851	3.547	3.303	3.283
Decision	Stable	Stable	OS	OS	OS
Decision Made at Sample	682	921	712	695	692
Decision Time, s	0.709	0.957	0.740	0.722	0.719

OS: Out-of-step

TABLE VIII
SUMMARY OF CLOSED-LOOP TESTING RESULTS FOR PRE-FAULT $\delta = 45°$ AND THE LINE TO GROUND FAULT APPLIED

Case	*29*	*30*	*31*	*32*	*33*
Fault Duration Time, s	0.6	0.68	0.683	0.684	0.7
Fault Duration Samples	577	653	656	657	673
Area (A_1), in 10^9	4.385	4.667	4.671	4.755	4.772
Area (A_2), in 10^9	4.391	4.669	4.671	1.806	1.777
Decision	Stable	Stable	Stable	OS	OS
Decision Made at Sample	821	1129	1246	957	937
Decision Time, s	0.853	1.174	1.295	0.995	0.974

OS: Out-of-step

It should also be noted that the units of A_1 and A_2 from hardware simulations are not *p.u.-s* (unlike in the software simulation results), as these values are obtained after scaling in the DSP. Accordingly, the areas A_1 and A_2 for hardware just represent numbers in the table. However, the ratio of A_1 to A_2 can still be used to compare the results using hardware and software. For example, for the case when fault duration time is 0.272 s, the ratio becomes 1.33 using hardware and 1.29 from software simulations, which are in good agreement. Another interesting point to note while comparing Fig. 21 and Fig. 24 is the nature of subsequent transient oscillations. In the case of Fig. 21 (RTDS result), the subsequent oscillations slightly increase in magnitude while in the case of Fig. 24 (PSCAD), the subsequent oscillations slightly decrease in magnitude and then remain as sustained out-of-step oscillations. In this case, the hardware result (RTDS) is a more accurate reflection of the actual behavior of the system compared to the software simulation result (PSCAD).

More testing results have been obtained with δ_0 set at 40° and 45°. Line to line fault ('a' phase to 'b' phase) and line to ground fault ('a' phase to ground) were applied and fault duration time varied. The area A_1, A_2, decision made and decision times are reported in the Tables VII–VIII.

The results obtained from the closed-loop testing were in close agreement with the results obtained from software simulations. The relay model developed showed that the proposed algorithm is simple to implement on digital hardware. The proposed algorithm was able to discriminate in cases well when the system was on the verge of instability. The successful real time testing using RTDS™ implied that the proposed relay can work effectively on an actual power system. The decision times obtained from the hardware testing were in accordance with those obtained from the software simulations. To account for measurement inaccuracies and the possibility of breaker re-closures, the decision times could be delayed by few sampling intervals (i.e., 0.00104 s or more), so that inaccurate decisions are avoided.

V. Conclusion

A technique for out-of-step detection by modifying the classical equal area criterion condition to the time domain was proposed in this paper and its effectiveness was tested on an SMIB and a three-machine infinite bus system. The proposed algorithm perfectly discriminated between stable and out-of-step swings based on the local voltage and current information available at the relay location. The analysis showed that the algorithm did not require line parameter information, and also did not require any off-line system studies. The proposed technique also does not need the inertia constant 'M' and is therefore more accurate than the classical $P-\delta$ equal area criterion, which requires the knowledge of 'M'. The simulation studies on a three-machine infinite bus configuration showed that the proposed algorithm can be directly applied to a multimachine system without any need for reduction of the system. Finally, closed-loop testing of the prototype of the relay using RTDS showed its applicability on an actual power system.

Appendix

SMIB Parameters:

Generator rating $= 4 * 555$ MVA, 24 kV
Direct axis transient reactance$(\mathrm{X}'_{\mathrm{d}}) = 0.3$
Inertia constant$(\mathrm{H}) = 3.5$ MW-s/MVA
Frequency $= 60$ Hz, infinite bus voltage $= 0.9$ p.u.
Transformer $=$ j 0.15 p.u., TL–I $=$ j0.5 p.u., TL–II $=$ j0.93 p.u.

Three-Machine Infinite Bus Parameters:

Generator–1 rating $= 555$ MVA, $\mathrm{H} = 3.38$ MW-s/MVA
Generator–2 rating $= 635$ MVA, $\mathrm{H} = 5.40$ MW-s/MVA
Generator–3 rating $= 66$ MVA, $(\mathrm{H}) = 4.29$ MW-s/MVA
Bus Voltage $= 24$ kV
$\mathrm{Z}_1 = 0.048 + j0.48\ \Omega, \mathrm{Z}_2 = 0.00576 + j0.573\ \Omega$
$\mathrm{Z}_3 = 0.0288 + j0.288\ \Omega, \mathrm{Z}_4 = 0.0576 + j0.576\ \Omega$
$\mathrm{Z}_5 = 0.0142 + j0.142\ \Omega, \mathrm{Z}_6 = 0.0192 + j0.192\ \Omega$
$\mathrm{Z}_7 = j0.0957\ \Omega$

Excitation System Parameters:

Exciter type: Field controlled alternator-rectifier excitation system (AC1A);
Lead time constant $(\mathrm{T_C}) = 0$ s, lag time constant $(\mathrm{T_B}) = 0$ s
Regulator gain $(\mathrm{K_A}) = 400$ p.u., time constant $(\mathrm{T_A}) = 0.02$ s
Max. regulator internal voltage $(\mathrm{V_{AMAX}}) = 14.5$ p.u.
Min. regulator internal voltage $(\mathrm{V_{AMIN}}) = -14.5$ p.u.
Underexcitation limit input signal = None
Overexcitation limit input signal = None
Max. regulator output voltage $(\mathrm{V_{RMAX}}) = 6.03$ p.u.
Min. regulator output voltage $(\mathrm{V_{RMIN}}) = -5.43$ p.u.
Rate feedback gain $(\mathrm{K_F}) = 0.03$ p.u.
Rate feedback time constant $(\mathrm{T_F}) = 1$ s
Exciter time constant $(\mathrm{T_E}) = 0.8$ s
Exciter constant related to field $(\mathrm{K_E}) = 1$ p.u.
Field current commutating reactance $(\mathrm{K_C}) = 0.2$ p.u.
Demagnetizing factor $(\mathrm{K_D}) = 0.38$ p.u.

Power System Stabilizer Parameters:

Stabilizer type: single input power system stabilizer (PSS1A);
Transducer time constant $(\mathrm{T_6}) = 0$ s, PSS Gain $(\mathrm{K_s}) = 5$ p.u.
Washout time constant $(\mathrm{T_5}) = 10$ s
Filter constant $(\mathrm{A_1}) = 0$, filter constant $(\mathrm{A_2}) = 0$
First lead time constant $(\mathrm{T_1}) = 0$ s,
First lag time constant $(\mathrm{T_2}) = 6$ s
Second lead time constant $(\mathrm{T_3}) = 0.08$ s
Second lag time constant $(\mathrm{T_4}) = 0.01$ s
PSS output limit, max. $(\mathrm{V_{RMAX}}) = 0.1$ p.u.
PSS output limit, Min. $(\mathrm{V_{RMIN}}) = -0.1$ p.u.

Governor Parameters:

Governor ued: Mechanical-hydraulic governor
Pilot valve servometer time constant $(\mathrm{T_P}) = 0.05$ s
Servo gin $(\mathrm{Q}) = 5$ p.u.,
Main servo time constant $(\mathrm{T_g}) = 0.2$ s
Temporary drop $(\mathrm{R_t}) = 0.4$ p.u.,
Reset time constant $(\mathrm{T_R}) = 5$ s
Permanent drop $(\mathrm{R_p}) = 0.04$ p.u.
Maximum gate position $(\mathrm{G_{min}}) = 1$ p.u.
Minimum gate position $(\mathrm{G_{max}}) = 0$ p.u.
Maximum gate opening rate $= 0.16$ p.u./s
Maximum gate closing rate $= 0.16$ p.u./s

EZ LITE-KIT Board Features:

One ADSP-BF533 Blackfin Processor;
Clock speed: 750 MHz;
32 MB (16M $\times$ 16-b) SDRAM, 2MB (512M $\times$ 16-b $\times$ 2) FLASH memory, AD1836 96 kHz audio codec with input and output RCA jacks, Three 90-pin connectors.

RTDS Features: The RTDS is a real-time digital power system simulator that mimics the actual power system in real time. The RTDS hardware is assembled in modular units called racks, and each rack is equipped with processing and communication modules. The RTDS simulator used for this study consists of a triple processor (3PC: Analog Devices' ADSP-21062 digital signal processor), a gigaprocessor (GPC: IBM PPC750GX PowerPC processors), a workstation interface card (WIF), 48 analog output ports (24 on 3PC and 24 on GPC), and a digital input interface (16 b).

Acknowledgment

The authors would like to thank Dr. D. Muthumuni and J. Carlos (Manitoba HVDC Research Centre) with the PSCAD software and H. Meiklejohn (RTDS Technologies, Winnipeg, MB, Canada) with the RSCAD software.

References

[1] W. A. Elmore, *Protective Relaying Theory and Applications*, 2nd ed. New York: Marcel Dekker, rev. and expanded. ed., 2004.
[2] C. R. Mason, *The Art and Science of Protective Relaying*. New York: Wiley, 1956.
[3] J. Holbach, "New out of step blocking algorithm for detecting fast power swing frequencies," in *Proc. Power Systems Conf.: Advanced Metering, Protection, Control, Communication, and Distributed Resources*, 2006, pp. 182–199.
[4] Y. Liu, "Aspects on power system islanding for preventing widespread blackout," in *Proc. IEEE Int. Conf. Networking, Sensing and Control*, 2006, pp. 1090–1095.

[5] A. Mechraoui, "A new principle for high resistance earth fault detection during fast power swings for distance protection," *IEEE Trans. Power Del.*, vol. 12, no. 4, pp. 1452–1457, Oct. 1997.
[6] D. Tziouvaras and D. Hou, "Out-of-step protection fundamentals and advancements," presented at the 30th Annu. Western Protective Relay Conf., Spokane, WA, Oct. 21–23, 2003.
[7] A. Y. Abdelaziz, "Adaptive protection strategies for detecting power system out-of-step conditions using neural networks," in *Proc. Inst. Elect. Eng., Gen., Transm. Distrib.*, 1998, vol. 145, pp. 387–394.
[8] W. Rebizant, "Fuzzy logic application to out-of-step protection of generators," in *Proc. IEEE Power Eng. Soc. Summer Meeting*, 2001, vol. 2, pp. 927–932.
[9] R. Padiyar and S. Krishna, "Online detection of loss of synchronism using energy function criterion," *IEEE Trans. Power Del.*, vol. 21, no. 1, pp. 46–55, Jan. 2006.
[10] V. Centeno, "An adaptive out-of-step relay [for power system protection]," *IEEE Trans. Power Del.*, vol. 12, no. 1, pp. 61–71, Jan. 1997.
[11] W. D. Stevenson, *Elements of Power System Analysis*, 4th ed. New York: McGraw-Hill, c1982.
[12] S. Cheng and M. S. Sachdev, "Out-of-step protection using the equal area criterion," in *Proc. Canadian Conf. Electrical and Computer Engineering*, 2005, pp. 1488–1491.
[13] P. Kundur, *Power System Stability Control*. New York: McGraw-Hill, 1994.
[14] PSCAD User Manuals Manitoba HVDC Research Centre. Winnipeg, MB, Canada.
[15] D. X. Du, "An advanced real time digital simulator based test system for protection relays," in *Proc. 41st Int. Univ. Power Eng.Conf.*, 2006, vol. 3, pp. 851–855.
[16] P. Forsyth, "Real time digital simulation for control and protection system testing," in *Proc. IEEE 35th Annu. Power Electronics Specialists Conf.*, 2004, vol. 1, pp. 329–335.
[17] IEEE Power System Relaying Committee of the IEEE Power Eng. Soc., Power swing and out-of-step considerations on transmission line. Rep. PSRC WG D6., Jul. 2005. [Online]. Available: http://www.pes-psrc.org/Reports/Power%20Swing%20and%20OOS%20Considerations%20on%20Transmission%20Lines%20F.pdf
[18] M. A. Pai, *Energy Function Analysis for Power System Stability*. Boston, MA: Kluwer, 1989.
[19] M. A. Pai, *Power System Stability :Analysis by the Direct Method of Lyapunov*. Amsterdam, The Netherlands: North-Holland, 1981.
[20] ADSP-BF533 EZ-KIT Lite Evaluation System Manual Analog Devices, Inc.

Sumit Paudyal (S'07) received the Bachelor's degree (B.E.) in electrical engineering (Hons.) from Tribhuvan University (T.U.), Kathmandu, Nepal, in 2003, the M.Sc. degree in electrical engineering from the University of Saskatchewan, SK, Canada, in 2008, and is currently pursuing the Ph.D. degree in electrical engineering at the University of Waterloo, Waterloo, ON, Canada.

He was a Research Assistant with Kathmandu Engineering College in 2003 and an Electrical Engineer with the Nepal Electricity Authority in 2004.

Gokaraju Ramakrishna (S'88–M'00) received the M.Sc. and Ph.D. degrees in electrical and computer engineering from the University of Calgary, Calgary, AB, Canada, in 1996 and 2000, respectively.

He is an Associate Professor at the University of Saskatchewan, Saskatoon, SK, Canada, and is currently Visiting Professor at the University of Manitoba, Winnipeg, MB, Canada. Prior to this appointment, he was a Graduate Engineer with Larsen and Toubro-ECC, India; Junior Research Fellow with the Indian Institute of Technology, Kanpur, India; Research Engineer with the Center of Intelligent Systems, Rourkela, India; Research Scientist with the Alberta Research Council, Canada; and Senior Staff Software Engineer with the IBM Toronto Lab, Toronto, ON, Canada. His areas of interest include power system control, protection, and applications of intelligent systems to power systems.

Mohindar S. Sachdev (S'63–M'67–SM'73–F'83–LF'97) was born in Amritsar, India, in 1928. He received the B.Sc. degree in electrical engineering from the Banaras Hindu University, Varanasi, India, in 1950, the M.Sc. degree from Punjab University, Chandigarh, India, and the University of Saskatchewan, Saskatoon, SK, Canada, and the Ph.D. and D.Sc. degrees from the University of Saskatchewan, Saskatoon.

He was with the Punjab P.W.D. Electricity Branch and the Punjab State Electricity Board from 1950 to 1968 in system operation, design, and planning. In 1968, he joined the University of Saskatchewan, where he is currently Professor Emeritus of Electrical Engineering. His areas of interest are power system analysis and power system protection.

Dr. Sachdev is a Fellow of the Institution of Engineers (India) and a Fellow of the Institution of Electrical Engineers (U.K.). He is also a Registered Professional Engineer in the Province of Saskatchewan and a Chartered Engineer in the U.K.